Inositol pyrophosphates regulate JMJD2C-dependent histone demethylation

Adam Burton[a,b], Cristina Azevedo[a,b], Catia Andreassi[b,c], Antonella Riccio[b,c,1], and Adolfo Saiardi[a,b,1]

[a]Medical Research Council Cell Biology Unit and Department of Cell and Developmental Biology, [b]Medical Research Council Laboratory for Molecular Cell Biology, and [c]Department of Neuroscience, Physiology, and Pharmacology, University College London, London WC1E 6BT, United Kingdom

Edited by Solomon H. Snyder, The Johns Hopkins University School of Medicine, Baltimore, MD, and approved October 11, 2013 (received for review May 27, 2013)

Epigenetic modifications of chromatin represent a fundamental mechanism by which eukaryotic cells adapt their transcriptional response to developmental and environmental cues. Although an increasing number of molecules have been linked to epigenetic changes, the intracellular pathways that lead to their activation/repression have just begun to be characterized. Here, we demonstrate that inositol hexakisphosphate kinase 1 (IP_6K1), the enzyme responsible for the synthesis of the high-energy inositol pyrophosphates (IP_7), is associated with chromatin and interacts with Jumonji domain containing 2C (JMJD2C), a recently identified histone lysine demethylase. Reducing IP_6K1 levels by RNAi or using mouse embryonic fibroblasts derived from *ip6k1*$^{-/-}$ knockout mice results in a decreased IP_7 concentration that epigenetically translates to reduced levels of trimethyl-histone H3 lysine 9 (H3K9me3) and increased levels of acetyl-H3K9. Conversely, expression of IP_6K1 induces JMJD2C dissociation from chromatin and increases H3K9me3 levels, which depend on IP_6K1 catalytic activity. Importantly, these effects lead to changes in JMJD2C-target gene transcription. Our findings demonstrate that inositol pyrophosphate signaling influences nuclear functions by regulating histone modifications.

inositides | phosphorylation | metabolism

Epigenetic modifications of histones are emerging as a central mechanism that controls nuclear functions, transducing changes in cell physiology to transcriptional reprogramming (1). Histones are subjected to numerous reversible posttranslational modifications, including acetylation, phosphorylation, methylation, ubiquitylation, ADP ribosylation, and sumoylation (2). Histone methylation has been associated with transcriptional control, mRNA splicing, DNA repair, and replication (3). Recently two families of histone demethylase enzymes have been identified in mammalian cells, lysine-specific demethylase 1 and the Jumonji-C domain-containing proteins (4, 5). The Jumonji-C histone demethylase family member, Jumonji domain-containing 2C (JMJD2C), removes trimethyl groups from lysines 9 and 36 of histone H3 by an oxidative reaction that requires iron and α-ketoglutarate as cofactors (6). Knockdown of JMJD2C decreased proliferation of tumor cells, whereas its expression in mammary epithelial cells induced a transformed phenotype (6, 7). JMJD2C is also an important mediator of embryonic stem-cell self-renewal via positive regulation of the key transcription factor Nanog (8).

Inositol pyrophosphates, including diphosphoinositol pentakisphosphate or PP-IP_5 (IP_7), belong to a specific class of inositol polyphosphates that undergo very rapid turnover (9, 10). They possess highly energetic pyrophosphate moieties that participate in phosphotransfer reactions (11, 12). Inositol pyrophosphates regulate many diverse cellular events (for review, see refs. 13–15) and this is likely to reflect their ability to control a very basic cellular function. In fact, recent discoveries indicate inositol pyrophosphates are master regulators of cell metabolism by controlling the balance between glycolysis and mitochondrial oxidative phosphorylation and thus ATP production (16), likely affecting cellular phosphate homeostasis (17, 18). This metabolic regulation is corroborated by the ability of inositol pyrophosphates to regulate insulin signaling (19) and accumulation of fat observed in ip6k1$^{-/-}$ mice (20). In mammalian cells, two classes of enzymes synthesize inositol pyrophosphates: the inositol hexakisphosphate kinases (IP_6Ks), which are able to phosphorylate the inositol ring at position five, generating the isomer 5PP-IP_5 of IP_7 (21), and the VIP1 (PP-IP_5K) family of enzymes, able to generate the 1PP-IP_5 isomer of IP_7 (22). Three IP_6K isoforms exist in the mammalian genome (23).

To further characterize the intracellular processes regulated by mammalian IP_6K1, we performed a yeast-two hybrid screen and identified JMJD2C as its interacting partner. The finding that the production of IP_7 by IP_6K1 affects JMJD2C functionality reveals a unique and critical role for inositol pyrophosphates in regulating mammalian epigenetic modifications.

Results

IP_6K1 Interacts with JMJD2C. We performed a yeast two-hybrid screen using the IP_6K1 N-terminal variable region as bait (amino acids 75–206), which we called the "Diff" region (Fig. S1). A number of proteins that regulate nuclear signaling and gene expression were identified, including the C-terminal region (amino acids 846–1,054) of the histone demethylase JMJD2C. Interestingly, this region specifically interacted with IP_6K1 (Diff1), but not with the homologous region of IP_6K2 (Diff2) (Fig. 1*A*). To test whether JMJD2C interacted with IP_6K1 in mammalian cells, HEK293T cells were transfected with JMJD2C-Flag and both GST-Diff1 and full-length GST-IP_6K1, and GST pull-down experiments were performed (Fig. 1*B*). We observed a robust interaction of JMJD2C-Flag and GST-IP_6K1. To assess the interaction of endogenous IP_6K1 with JMJD2C, we generated an IP_6K1 antibody, which specifically recognizes IP_6K1

Significance

Epigenetic modifications of chromatin are emerging as important regulatory mechanisms of many nuclear processes. Numerous proteins have been identified that mediate these modifications in a dynamic manner. However, less is known about the signaling pathways that transduce upstream signals into chromatin changes. Here, we show that the signaling molecule inositol pyrophosphate (IP_7) synthesised by inositol hexakisphosphate kinase 1 plays a key role in regulating the association of one of these proteins, Jumonji domain containing 2C with chromatin, thereby controlling the levels of a number of crucial epigenetic modifications important to regulate gene expression.

Author contributions: A.B., A.R., and A.S. designed research; A.B., C. Azevedo, and C. Andreassi performed research; C. Azevedo, C. Andreassi, and A.R. contributed new reagents/analytic tools; A.B., C. Azevedo, C. Andreassi, A.R., and A.S. analyzed data; and A.B., A.R., and A.S. wrote the paper.

The authors declare no conflict of interest.

This article is a PNAS Direct Submission.

[1]To whom correspondence may be addressed. E-mail: dmcbado@ucl.ac.uk or a.riccio@ucl.ac.uk.

This article contains supporting information online at www.pnas.org/lookup/suppl/doi:10.1073/pnas.1309699110/-/DCSupplemental.

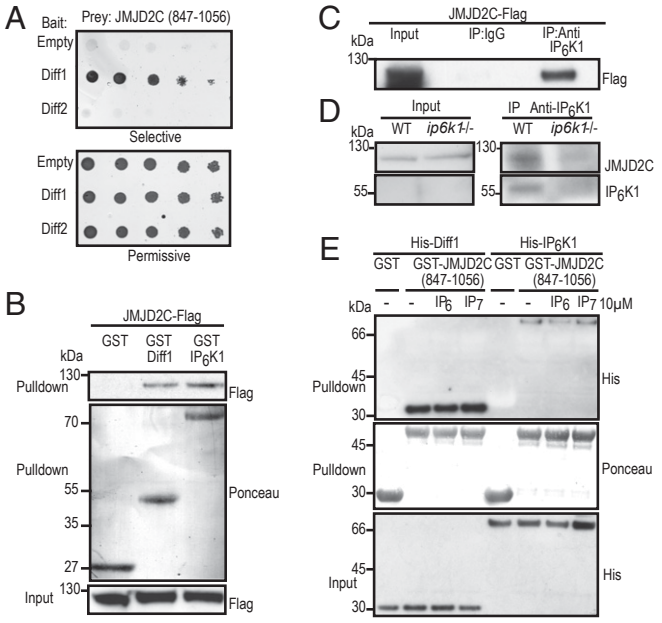

Fig. 1. IP_6K1 and JMJD2C are binding partners in vitro and in vivo. (*A*) IP_6K1 (Diff) interacts with JMJD2C (847–1,056) by yeast two-hybrid. Yeast reporter strain AH109 was cotransformed either with empty pGBKT7, pGBKT7-Diff1, or pGBKT7-Diff2 and pACT2-JMJD2C (847–1,056). Serial dilution of yeast grown on selective media to assess interaction strength (*Upper*) or permissive media (*Lower*) and grown at 30 °C for 3 d ($n = 3$). (*B*) Immunoblot analysis of HEK293T cells transfected with JMJD2C-Flag and either GST-IP_6K1, GST-Diff, or GST empty vector control and subjected to GST pull-down assays. The Ponceau staining confirmed the pull-down of the GST-tagged proteins ($n = 3$). (*C*) Immunoblot analysis of HEK293T cells transfected with JMJD2C-Flag and subjected to coimmunoprecipitation with anti-IP_6K1 antibody. The blot was probed with anti-FLAG antibody ($n = 3$). (*D*) MEF cell extracts from either wild-type (WT) or IP_6K1 null (*ip6k1*$^{-/-}$) mice were subjected to coimmunoprecipitaton with Sepharose-conjugated anti-IP_6K1 antibody and probed with either anti-JMJD2C or anti-IP_6K1 antibodies ($n = 3$). (*E*) Recombinant GST-JMJD2C (847–1,056) or GST were subjected to in vitro binding assays either with recombinant His-Diff1 or His-IP_6K1 in the presence of 10 μM IP_6 or IP_7. Pull-downs and 5% of the inputs were immunoblotted with anti-His antibody and Ponceau staining demonstrates pull-down of the GST-tagged proteins ($n = 3$).

in WT but not in knockout (*ip6k1*$^{-/-}$) mouse brain extracts (24) (Fig. S2 *A* and *B*). Although in mouse embryonic fibroblasts (MEFs) the level of IP_6K1 is below detection level by Western blot analysis, the antibody worked well in immunoprecipitation assays revealing a band at the expected molecular size of IP_6K1 in WT but not in *ip6k1*$^{-/-}$ MEF extracts (Fig. S2*C*). Importantly, our IP_6K1 antibody was also capable of coimmunoprecipitating both Flag-JMJD2C (Fig. 1*C*) and the endogenous JMJD2C protein (Fig. 1*D*). We next investigated whether IP_6K1 directly interacted with JMJD2C by performing pull-down experiments in vitro using recombinant, bacterial-expressed proteins (Fig. 1*E*). Purified GST-JMJD2C (amino acids 847–1,056) pulled down both His-Diff1 and full-length His-IP_6K1, and their interaction in vitro was not affected by IP_6 or IP_7.

IP_6K1 Is Associated with Chromatin. JMJD2C is a histone demethylase that is mostly localized in the nucleus (6). Because neither the IP_6K1 antibody nor the commercially available JMJD2C antibodies are suitable for immunohistochemistry analysis, we characterized IP_6K1 intracellular localization by expressing GFP-IP_6K1 and JMJD2C-Flag in mammalian cells, with both proteins specifically detected in the nucleus of HeLa cells (Fig. S3). To address the localization of endogenous IP_6K1 in more detail, subcellular fractionation experiments were performed. Nuclear partition into nucleoplasmic and chromatin fractions revealed the presence of endogenous IP_6K1 in both compartments, demonstrating that IP_6K1 is found in association with chromatin (Fig. 2*A*). Coimmunoprecipitation experiments performed on lysates of MEFs treated with DNase showed that histone H3 coimmunoprecipitated with IP_6K1 in wild-type MEFs, but not in MEFs obtained from *ip6k1*$^{-/-}$ mice (24) (Fig. 2*B*). IP_6K1 also coimmunoprecipitated trimethyl-H3K9 (H3K9me3), a methylated histone substrate of JMJD2C (Fig. 2*C*), but failed to coimmunoprecipitate trimethyl-H3K36 (H3K36me3) (Fig. S4) a second methylated histone substrate of JMJD2C. These data suggest that IP_6K1 is able to associate specifically with H3K9me3-containing chromatin regions to which JMJD2C is targeted. To further characterize the interaction of IP_6K1 with chromatin, we performed in vitro binding assays of IP_6K1 and found that (Fig. 2*D*) IP_6K1 directly interacts with histone H3, providing a mechanism for the recruitment of IP_6K1 to chromatin.

Inositol Pyrophosphate Regulates H3K9me3 Levels. The H3K9me3 modification, removed by JMJD2C, is an epigenetic mark associated with euchromatic transcriptional silencing and heterochromatin formation (2, 25). To test whether the interaction of IP_6K1 with JMJD2C induced epigenetic changes, we assessed the global levels of H3K9me3 in cells lacking IP_6K1. Somewhat surprisingly, in MEFs obtained from *ip6k1*$^{-/-}$ mice, we detected a markedly reduced level of global H3K9me3, compared with wild-type MEFs, whereas total histone H3 levels remained unchanged (Fig. 3*A*). Expression of GST-IP_6K1 in *ip6k1*$^{-/-}$ cells restored H3K9me3 to wild-type levels. Furthermore, expression of GST-IP_6K1 in wild-type MEFs caused an additional increase of H3K9me3 levels (Fig. 3*A*). Histone posttranslational modifications mostly occur in clusters located within histone N-terminal tails. Lysine 9 and serine 10 of histone H3 represent one of the "hot spots" for posttranslational modifications. In transcriptionally active genes, acetylation of H3 on lysine 9 correlates with serine 10 phosphorylation (2), opposing lysine 9 methylation and thereby acting as a "binary switch" of transcriptional regulation (26). We next tested whether the levels of these modifications were also altered in cells lacking IP_6K1. Consistently, global levels of acteyl-H3K9 were dramatically increased in *ip6k1*$^{-/-}$ MEFs, compared with wild-type cells (Fig. 3*A*). This

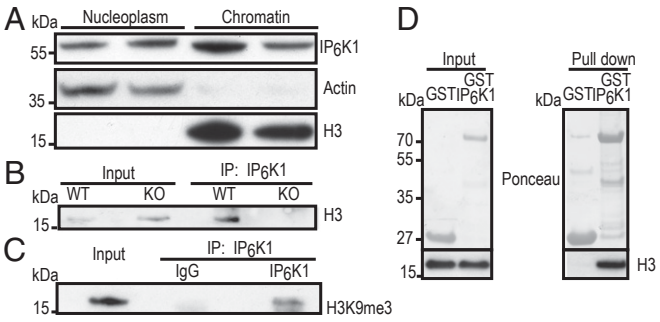

Fig. 2. Nuclear localization and chromatin association of IP_6K1. (*A*) IP_6K1 associates with chromatin. HEK293T nuclear pellets were subjected to fractionation into soluble (nucleoplasm) and chromatin fractions. Immunoblotting was subsequently performed with antibodies to actin and histone H3 as quality controls and anti-IP_6K1. (*B*) IP_6K1 associates with histone H3. MEF cells from wild-type (WT) and IP_6K1 knockout (*ip6k1*$^{-/-}$) mice were subjected to coimmunoprecipitaton with anti-IP_6K1 antibody after DNase treatment of lysates. Pull-downs and 5% inputs were separated by SDS/PAGE and membranes were subsequently blotted with anti-histone H3 antibody. (*C*) IP_6K1 associates with chromatin bearing the H3K9me3 mark. Coimmunoprecipitation with anti-IP_6K1 was performed on DNase-treated HEK293T lysates. Inputs and immunoprecipitated samples were separated by SDS/PAGE and blotted with anti-H3K9me3 antibody. (*D*) IP_6K1 associates with histone H3. In vitro binding assays were performed with recombinant GST-IP_6K1 and purified H3.1 protein.

CELL BIOLOGY

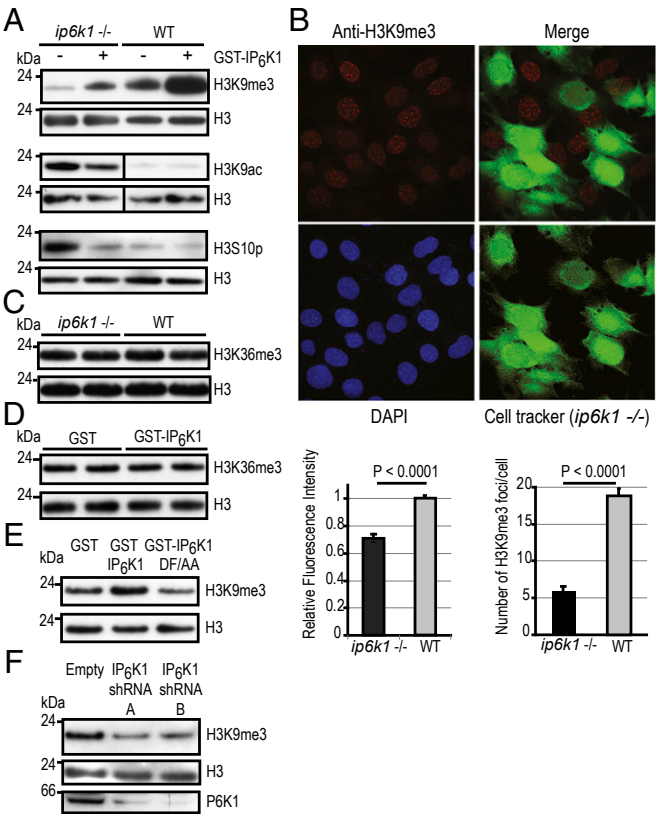

Fig. 3. IP_6K1 catalytic activity regulates epigenetic modifications of histone H3 at the K9/S10 hot-spot. (*A*) IP_6K1 knockout MEFs (*ip6k1*$^{-/-}$) display reduced levels of H3K9me3 and increased levels of both acetyl-H3K9 and phospho-H3S10, which can be rescued by expression of IP_6K1. In the case of the acetyl-H3K9, a dividing line is shown to indicate that nonessential lanes were removed from the single original blot. Immunoblots of cell extracts obtained either from *ip6k1*$^{-/-}$ or WT MEFs and probed with the corresponding antibodies. The experiments were performed at least three times with two independent lines of WT and *ip6k1*$^{-/-}$ MEFs. (*B*) Immunohistochemistry of *ip6k1*$^{-/-}$ MEFs confirms reduced levels of H3K9me3. MEFs obtained from *ip6k1*$^{-/-}$ mice were labeled with cell tracker (green), mixed with WT MEFs, and immunostained with anti-H3K9me3 antibody (red). Images were taken on a Leica TCS SPE confocal microscope and quantified using LAS AF software (Leica). *Left* graph represents the mean ±SE of the average H3K9me3 fluorescence intensity of 97 KO and 68 WT cells ($n = 3$). *Right* graph represents the mean ±SE of the number of H3K9me3 foci per nuclei of 77 KO and 74 WT cells. Statistical analysis was performed using the Mann–Whitney *u* test. (Scale bar, 30 μm.) ($n = 3$). (*C*) Immunoblot analysis of H3K36me3 shows no difference between WT and *ip6k1*$^{-/-}$ MEFs ($n = 4$). (*D*) Immunoblot of HEK293T cells expressing GST-IP_6K1 and analyzed for H3K36me3 mark ($n = 3$). (*E*) Immunoblot analysis of HEK293T cells expressing either GST-IP_6K1 or the catalytically inactive mutant GST-IP_6K1 (DF/AA) and analyzed for H3K9me3 mark ($n = 4$). (*F*) H3K9me3 immunoblot of HEK293T cells depleted of IP_6K1 for 48 h by using two short hairpin RNAs (shRNA-A and shRNA-B) ($n = 3$).

effect was partially rescued by expressing GST-IP_6K1 in *ip6k1*$^{-/-}$ MEFs. Similarly, increased levels of phospho-H3S10 were detected in *ip6k1*$^{-/-}$ MEFs compared with wild type, and normal phospho-H3S10 levels were recovered by expressing GST-IP_6K1. To further confirm these findings, immunofluorescence studies were performed. A highly significant (29 ± 3%) decrease in the level of staining of H3K9me3 was observed in *ip6k1*$^{-/-}$ MEFs, compared with the wild-type cells (Fig. 3*B*). Interestingly, H3K9me3 nuclear staining appeared more diffuse in *ip6k1*$^{-/-}$ MEFs, as shown by the dramatic decrease (68 ± 3%) of H3K9me3 from DAPI-dense heterochromatin foci (Fig. 3*B*). Taken together these findings demonstrate that IP_6K1 exerts a dramatic effect on chromatin modifications, particularly at the K9/S10 binary switch, via an inhibitory effect on the histone demethylase JMJD2C.

In addition to H3K9me3, JMJD2C also demethylates trimethyl-H3 lysine 36 (H3K36me3), an epigenetic mark associated with transcriptional elongation (27). In contrast to H3K9me3, in *ip6k1*$^{-/-}$ MEFs H3K36me3 levels were not altered (Fig. 3*C*). Similarly, when GST-IP_6K1 was expressed in HEK293T cells, H3K36me3 levels remained unchanged (Fig. 3*D*). The apparent inability of IP_6K1 to alter H3K36me3 levels likely reflects the absence of localization of this kinase at the H3K36me3 chromatin loci (Fig. S4) and thus lack of local inositol pyrophosphate synthesis. Because the conserved tandem Tudor domains of the closely related demethylase JMJD2A were reported to bind both H3K4me3 and H4K20me3 (28), we tested H3K4me3 and H4K20me3 levels in *ip6k1*$^{-/-}$ MEFs. No difference between wild-type and *ip6k1*$^{-/-}$ MEFs was observed. Thus, IP_6K1 associates with and regulates the specific state of posttranslational modifications at the K9/S10 hot spot of histone H3, rather than affecting histone methylation in general.

We next investigated whether IP_6K1-mediated epigenetic changes depended on IP_6K1 enzymatic activity. GST-IP_6K1 was expressed in HEK293T cells, and H3K9me3 levels were assessed (Fig. 3*E*). As expected, expression of wild-type GST-IP_6K1 increased global levels of H3K9me3 by more than twofold, compared with cells expressing empty vector controls, further demonstrating that IP_6K1 regulates H3K9me3 levels (Fig. 3*E* and Fig. S5). Importantly, in cells transfected with a catalytically inactive form of IP_6K1 (DF/AA) (29), the levels of H3K9me3 remained unchanged (Fig. 3*E* and Fig. S4). Moreover, similarly to the HEK293T cells, in the *ip6k1*$^{-/-}$ MEFs transfected with the catalytically inactive form of IP_6K1 (DF/AA), the levels of H3K9me3 remained unchanged (Fig. S6). In contrast, increased levels of H4K9me3 were observed when cells were transfected with catalytically active IP_6K1 (Fig. S6). Furthermore, reduced levels of H3K9me3 were also observed in HEK293T cells transfected with two specific shRNAs that targeted IP_6K1 (Fig. 3*F*).

These data suggest that the inositol pyrophosphate synthesis catalyzed by IP_6K1 is necessary to mediate the increase in histone H3 methylation. Alternatively, IP_6K1 might directly affect the phosphorylation status of either histone H3 or JMJD2C, thereby changing its activity. To test this hypothesis we incubated IP_6K1 with either histone H3, JMJD2C, or IP_6, as substrates (Fig. S7). Although we observed a robust phosphorylation of IP_6 to IP_7, no transfer of phosphate to the two protein substrates was detected (Fig. S7).

Because the catalytic activity of IP_6K1 was required to mediate the increased global H3K9me3 levels, we investigated the nature of the inositol pyrophosphate species that regulate JMJD2C-dependent histone demethylation. IP_6Ks enzymes synthesize 5PP-IP_5, whereas the PP-IP_5Ks enzymes phosphorylate the 1 positions of IP_6 to generate the isomer 1PP-IP_5 of IP_7 and 1,5(PP)$_2$-IP_4 (IP_8) (22). The expression of Myc-PP-IP_5K1 in HEK293T cells increased IP_8 levels (Fig. S8 *A* and *B*) without affecting the level of H3K9me3 (Fig. S8*C*). These results indicate that it is the 5PP-IP_5 isomer of IP_7 synthesized by IP_6K1 that specifically regulates H3K9 methylation.

Inositol Pyrophosphates Regulate JMJD2C Chromatin Association. We next tested whether 5PP-IP_5 influences histone H3 modifications in a JMJD2C-dependent manner. The effect of IP_6K1 overexpression on H3K9 methylation was assessed in cells depleted of JMJD2C. HEK293T cells were transfected with two distinct siRNAs specific to JMJD2C, and knockdown of JMJD2C protein levels was confirmed by Western blot analysis (Fig. 4*A*). Cells with low levels of JMJD2C showed an increase of global H3K9me3, and this effect was rescued by expressing a mouse JMJD2C cDNA that was not targeted by the siRNAs (Fig. 4*A*). Importantly, when catalytically active IP_6K1 was expressed in cells with reduced levels of JMJD2C, we did not observe any further increase of H3K9me3 levels over cells expressing inactive

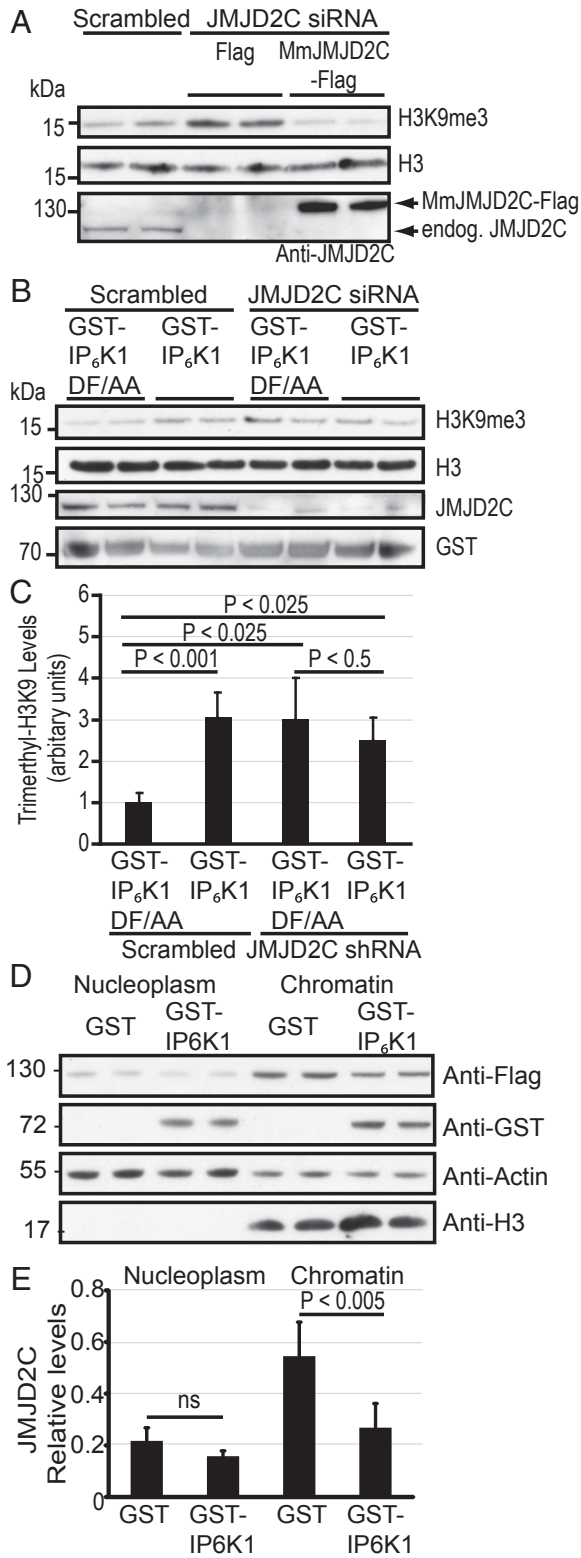

Fig. 4. Inositol pyrophosphates regulate histone modifications through JMJD2C chromatin association. (*A*) JMJD2C protein levels were reduced in human HEK293T cells with two different specific siRNAs for 96 h. *Mus musculus* (Mm) JMJD2C was expressed 16 h before cells were lysated and immunoblotting performed. (*B*) The effect of IP_6K1 kinase activity on H3K9me3 levels depends on JMJD2C. Cells were transfected with JMJD2C siRNAs as above and subsequently transfected either with GST-IP_6K1 or GST-IP_6K1 DF/AA, 16 h before analysis. Total proteins were extracted, separated by SDS/PAGE, and blots were probed with the indicated antibodies. Experiments were performed two times in duplicate. The increase in H3K9me3 levels relative to total histone H3 observed between lanes 3 and 4 over lanes 1 and 2 is no longer apparent in the context of JMJD2C knockdown, now comparing lanes 7 and 8 to lanes 5 and 6. (*C*) Quantitative analysis of histone H3K9me3 levels normalized to total histone H3. Average ± SEM of the four experiments is shown. The Mann–Whitney *u* test was used to determine statistical significance. (*D*) IP6K1 induces dissociation of JMJD2C from chromatin. HEK293T cells were transfected with either empty GST or GST-IP_6K1 and JMJD2C-Flag, and nuclear extracts were separated into chromatin or nucleoplasmic fractions. Western blot analyses were performed with anti-Flag, anti-GST, anti-histone H3, and anti-actin antibodies. (*E*) Quantitative analysis of JMJD2C levels normalized to actin or histone H3 for nucleoplasm or chromatin, respectively. NS, nonsignificant. Average ± SD of two experiments both run in duplicate is shown. The Mann–Whitney *u* test was used to determine statistical significance.

IP_6K1 (Fig. 4*B*, compare lanes 5 and 6 to 7 and 8), an activity-dependent k9me3 increase normally observed (Fig. 4*B*, compare lanes 1 and 2 to 3 and 4; see also Fig. 3*E* and Fig. S5). This effect was quantified across four independent experiments, demonstrating that the increased H3K9me3 levels observed after expression of catalytically active IP_6K1 were dependent on the presence of JMJD2C (Fig. 4*C*). Taken together, these results show that the IP_6K1-dependent increase of H3K9me3 is mediated via inhibition of JMJD2C and through the synthesis of IP_7. It should be noted, however, that addition of either 5PP-IP_5 or 1/3PP-IP_5 (both isomers of IP_7) did not change JMJD2C demethylase activity, when assayed in vitro using the purified catalytic domain of JMJD2C (12–349) (30) (Fig. S9), thereby suggesting that the effect of inositol pyrophosphates on JMJD2C is not mediated by a direct inhibition of its demethylase activity.

We next addressed how inositol pyrophosphates regulate JMJD2C demethylase activity. Although neither JMJD2C nor histones themselves are targets of IP_7-mediated pyrophosphorylation, we observed a number of chromatin-associated proteins that appeared to be its bona fide substrates (Fig. S10). It is possible that IP_7-dependent pyrophosphorylation regulates the assembly and/or stability of multiprotein complexes associated with chromatin, thereby influencing JMJD2C recruitment and consequently its demethylase activity. To test whether IP_6K1 affects the association of JMJD2C with chromatin, nuclear fractionation experiments were performed in HEK293T cells expressing either GST alone or GST-IP_6K1 and JMJD2C-Flag. Both IP_6K1 and JMJD2Cwere clearly detectable in the chromatin fraction, as expected (Fig. 4*D*). In contrast, JMJD2C more readily dissociated from the chromatin of cells transfected with IP_6K1 (Fig. 4 *D* and *E*). To test whether JMJD2C chromatin association depends on IP_7 synthesis or it is mediated via a steric effect, nuclear fractionation experiments were performed in cells expressing either GST-IP_6K1 or IP_6K1 DF/AA. There was a stronger dissociation of JMJD2C from the chromatin in cells transfected with the active IP_6K1 (Fig. S11), confirming that JMJD2C chromatin association depends on IP_6K1 catalytic activity. These results are in agreement with the IP6K1 activity-dependent influence toward the levels of histone H3K9 trimethylation. The observed decreased level of active IP_6K1 chromatin association (Fig. S11) is coherent with a model involving an IP_7-dependent dissociation of the entire IP_6K1-JMJD2C complex.

Inositol Pyrophosphates Regulate JMJD2C-Dependent Transcription. To test whether IP_6K1 and IP_7 regulate epigenetic changes at JMJD2C-dependent promoters, we performed chromatin immunoprecipitation assays (ChIPs). The Mdm2 oncogene was analyzed, as the promoter of this gene has been shown to be directly bound by and its expression up-regulated by JMJD2C demethylase activity (31). IP_6K1 was also observed on the Mdm2 P2 promoter in MEFs obtained from wild-type mice (Fig. 5*A*). In agreement with our Western blot and fractionation analyses, in MEFs isolated from *ip6k1*$^{-/-}$ mice, levels of H3K9me3 on the Mdm2 P2 promoter were lower, whereas levels of JMJD2C were

CELL BIOLOGY

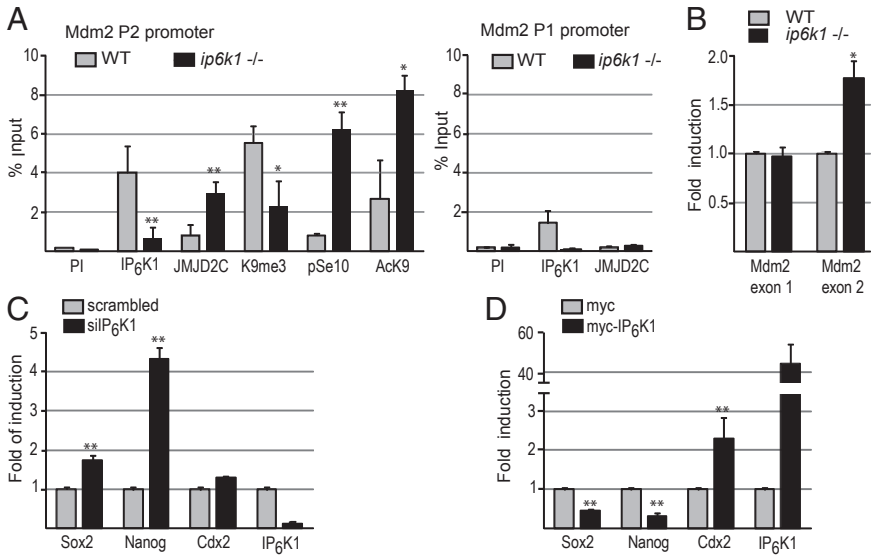

Fig. 5. Inositol pyrophosphates control the expression of JMJD2C-regulated genes. (*A*) Chromatin immunoprecipitation analysis of MEFs obtained either from WT or *ip6k*$^{-/-}$ mice. IP_6K1, H3K9me3, JMJD2C, H3S10ph, and H3K9ac immunoprecipitation followed by qPCR of either P1 or P2 promoters of the JMJD2C-regulated gene Mdm2. PI, preimmune serum. Data are represented as percentage of total input. Shown are the averages ±SEM. Parried Student *t* test was applied to calculate the statistical significance of the value of the *ip6k1*$^{-/-}$ against WT ($n = 3$; $*P < 0.01$, $**P < 0.001$). (*B*) IP_6K1 regulates levels of Mdm2 expression from exon 2 but not exon 1. qRT-PCR of mRNA extracted from either WT or *ip6k*$^{-/-}$ MEF. Mdm2 exon 1 and exon 2 mRNA was normalized to 18S ribosomal RNA ($n = 3$; $*P < 0.01$). (*C* and *D*) IP_6K1 regulates expression of JMJD2C-dependent genes in embryonic stem (ES) cells. (C) Specific siRNA to IP_6K1 or scrambled siRNA were transfected in embryonic stem cells in two rounds of transfection. RNA was extracted 24 h after the second transfection and analyzed by qRT-PCR ($n = 3$; $**P < 0.001$). (*D*) Myc-IP_6K1 or empty vector controls were transfected into ES cells and after 48 h RNA was extracted and subjected to qRT-PCR. Levels of Nanog, Sox2, and Cdx2 cDNA were normalized to actin and GAPDH and expressed as fold induction over control samples ($n = 3$; $**P < 0.001$).

higher, compared with WT cells (Fig. 5*A*). Furthermore, phospho-H3S10 and acetyl-H3K9 levels around Mdm2 P2 promoter were significantly higher in *ip6k1*$^{-/-}$ MEFs, compared with WT MEFs. As a control, the binding of JMJD2C and IP_6K1 to the Mdm2 P1 promoter was tested. As previously reported (31) JMJD2C does not bind the Mdm2 P1 promoter (Fig. 5*A*) and extremely low levels of IP_6K1 were also detected on the P1 promoter in WT MEFs (Fig. 5*A*). Importantly, in *ip6k1*$^{-/-}$ MEFs, the low levels of H3K9me3 and high H3K9ac observed around the Mdm2 P2 promoter correlated with increased transcription of Mdm2 exon 2 (Fig. 5*B*). To further substantiate the hypothesis that IP_6K1 plays a key role in regulating JMJD2C-dependent transcription, the expression levels of genes known to be controlled by JMJD2C were analyzed in mouse embryonic stem cells (8). In ES cells, both knockdown and overexpression of IP_6K1 induced significant changes in both Nanog and Sox2 expression (Fig. 5 *C* and *D*). Moreover, overexpression of IP_6K1 up-regulated basal levels of Cdx2 48 h posttransfection (Fig. 5*D*).

Discussion

We have identified a distinctive functional link between inositol phosphate intracellular signaling and the regulation of histone modifications at the functionally important residue lysine 9 of histone H3. The regulation of the histone demethylase JMJD2C association with chromatin by IP_6K1 via the production of the 5PP-IP_5 isomer of IP_7 introduces a unique scenario for inositol pyrophosphate signaling, indicating that these high-energy molecules play a fundamental role in mediating mammalian nuclear processes. Indeed the direct binding of IP_6K1 to chromatin, and the regulation of expression of a variety of JMJD2C-dependent genes including both Mdm2 and a number of crucial transcription factors in embryonic stem cells, highlights the important functional role of IP_6K1 and inositol pyrophosphates in controlling gene expression. Several mitochondrial metabolites like ATP, α-ketoglutarate, or acetyl-CoA play a key role in regulating epigenetic changes because these metabolites are cofactors for several epigenetic modifier enzymes (32, 33). Jumonji-C histone demethylases require α-ketoglutarate to perform their demethylase activity. Inositol pyrophosphates are able to control cellular energetic metabolism by regulating mitochondrial physiology (16) and are likely to affect the cellular levels of the metabolites required by the epigenetic modifier enzymes. Thus, inositol pyrophosphates may control the epigenetic program at an additional level besides regulating JMJD2C association to chromatin as we have demonstrated in the current work.

Interestingly IP_6K1 does not affect trimethylation of lysine 36 of histone H3, a second substrate of JMJD2C demethylase activity. Absence of IP_6K1 association with H3K36me3-containing chromatin regions, and thus the lack of local inositol pyrophosphates synthesis, explains the inability of IP_7 to regulate JMJD2C activity at these loci. Our data are in agreement with a previous report observing a differential regulation of H3K9me3 versus H3K36me3 by JMJD2C in regulating hypoxia-inducible factor 1 (HIF-1)-controlled transcription (34).

Inositol pyrophosphates may act in concert with phosphoinositide lipids, which are emerging as important regulators of nuclear signaling (35, 36). The presence of two plant homeodomain (PHD) finger domains in the JMJD2C sequence suggest that this protein might interact with phosphoinositides. The binding of phosphoinositides to PHD finger-domain–containing proteins in the nucleus has been proposed to regulate subnuclear localization of these proteins (37).

The region of JMJD2C found to interact with IP_6K1 contains tandem TUDOR domains, which have been implicated in protein–protein interactions with methylated protein substrates. Indeed, the tandem TUDOR domains of the closely related histone demethylase JMJD2A have been shown to bind H3K4me3 and H4K20me3. If, as it is likely, the highly conserved TUDOR domains of JMJD2C also mediate binding to these or other histone methylation marks, it is noteworthy that the binding site of IP_6K1 is also located within this region of JMJD2C. However, the inhibitory effect of IP_6K1 on the chromatin association of JMJD2C is unlikely to be due to a direct steric obstruction as it is clearly dependent on the catalytic activity of IP_6K1. It is likely that the inhibitory effect of inositol pyrophosphates on the binding of JMJD2C to chromatin is dependent on the native chromatin environment and the multiprotein complexes also found at these sites.

Histone demethylases are dynamic regulators of chromatin epigenetic status and their activity has been linked to numerous cellular processes (38). The methylation state of H3K9 correlates with the affinity for heterochromatic proteins that influence chromosomal organization and stability (39). JMJD2C has been shown to regulate tumorigenesis (6, 7), embryonic stem-cell self-renewal (8), and androgen receptor-dependent gene expression (30). The role of IP_6K1 in regulating expression of JMJD2C-target genes implicates both this enzyme and inositol pyrophosphates in the

same processes. In particular, the effect of IP_6K1 on the expression of genes important for embryonic stem-cell self-renewal uncovers a unique, yet unexplored function for inositol pyrophosphate signaling.

Mice lacking IP_6K1 are significantly smaller than wild type, indicating a possible developmental defect, and male mice lacking IP_6K1 are sterile due to defects in spermatogenesis (27), a process in which histone epigenetic modifications play a crucial role (40). Interestingly, disruption of the H3K9me3 histone methyltransferases SUV39H1 and -2 in mice also results in severe hypogonadism and spermatogenesis defects as well as abnormal heterochromatin formation (41). Our discovery that IP_6K1 is an endogenous regulator of JMJD2C and H3K9 methylation strongly suggests that inositol pyrophosphates play an important role in regulating the epigenetic modifications associated with these processes.

Materials and Methods

RNA Extraction, cDNA Synthesis, and Quantitative PCR Analysis of Gene Expression Levels in Embryonic Stem Cells and MEFs. RNA was extracted using the NucleoSpin RNA II kit (Macherey-Nagel) according to the manufacturer's instructions. cDNA synthesis was performed using the M-MLV Reverse Transcriptase kit (Invitrogen) according to the manufacturer's instructions. Relative cDNA content was analyzed using 1× Sybr Green PCR mix, 200 nM of primers, and 100 ng of cDNA in a 20-μL reaction on a Roche LightCycler 480 system. For experiments performed with MEFs, normalization was performed using the Ambion Quantitation RNA Universal 18S kit. Primers and detailed RT-PCR conditions are available upon request.

Chromatin Binding and Chromatin Immunoprecipitation. The procedure for the chromatin binding experiments was adapted from (42). Briefly, cells were suspended in a solution containing 50 mM Tris·HCl (pH 7.5), 0.5% Triton X-100, 300 mM NaCl, 60 mM $MgCl_2$, 10 mM $CaCl_2$, and DNase I (167 units·mL^{-1}; Roche) to solubilize histone H3 from the chromatin, and incubated at 30 °C for 50 min. Samples were sonicated 3 × 5 s at setting 1.5 on a Branson Sonifier 450 (Branson Ultrasonics Co.) and cleared by centrifugation at 15,000 × *g* for 10 min. The supernatants were diluted 1:2 with H_2O and added to the equilibrated glutathione or protein A or G Sepharose beads and GST pull-down or immunoprecipitations proceeded as described above. ChIP assay was performed as previously described with minor modifications (43). Primer sequences and PCR conditions are available upon request.

Quantitative PCR (25 μL) contained 12.5 μL of PCR Sybr Green mix (NEB) and 0.3 mM primers. All reactions were performed in duplicate on an Opticon 2 system (MJ Research) and each experiment included a standard curve, a preimmune control, and a no-template control. Standard templates consisted of gel-purified PCR products of *Mdmd2* P1 and P2 promoter amplicons of known concentration and each standard curve consisted of eight serial dilutions of template. At the end of 46 cycles of amplification, a dissociation curve was performed in which Sybr Green was measured at 1 °C intervals between 50 °C and 100 °C. Melting temperatures for *Mdmd2* P1 and P2 were 79 °C and 87 °C, respectively. Results were expressed as percentage of total input.

A full description of the methods used in this study can be found in *SI Materials and Methods*.

ACKNOWLEDGMENTS. We are grateful to Dr. Steve Shears for providing the PP-IP_5K plasmid. This work was supported by the Medical Research Council (MRC) funding to the Cell Biology Unit and by Human Frontier Science Program Grant RGP0048/2009-C.

1. Aguilar-Arnal L, Sassone-Corsi P (2013) The circadian epigenome: How metabolism talks to chromatin remodeling. *Curr Opin Cell Biol* 25(2):170–176.
2. Kouzarides T (2007) Chromatin modifications and their function. *Cell* 128(4):693–705.
3. Martin C, Zhang Y (2005) The diverse functions of histone lysine methylation. *Nat Rev Mol Cell Biol* 6(11):838–849.
4. Shi Y, et al. (2004) Histone demethylation mediated by the nuclear amine oxidase homolog LSD1. *Cell* 119(7):941–953.
5. Tsukada Y, et al. (2006) Histone demethylation by a family of JmjC domain-containing proteins. *Nature* 439(7078):811–816.
6. Cloos PA, et al. (2006) The putative oncogene GASC1 demethylates tri- and dimethylated lysine 9 on histone H3. *Nature* 442(7100):307–311.
7. Liu G, et al. (2009) Genomic amplification and oncogenic properties of the GASC1 histone demethylase gene in breast cancer. *Oncogene* 28(50):4491–4500.
8. Loh YH, Zhang W, Chen X, George J, Ng HH (2007) Jmjd1a and Jmjd2c histone H3 Lys 9 demethylases regulate self-renewal in embryonic stem cells. *Genes Dev* 21(20): 2545–2557.
9. Burton A, Hu X, Saiardi A (2009) Are inositol pyrophosphates signalling molecules? *J Cell Physiol* 220(1):8–15.
10. Shears SB (2009) Diphosphoinositol polyphosphates: Metabolic messengers? *Mol Pharmacol* 76(2):236–252.
11. Saiardi A, Bhandari R, Resnick AC, Snowman AM, Snyder SH (2004) Phosphorylation of proteins by inositol pyrophosphates. *Science* 306(5704):2101–2105.
12. Azevedo C, Burton A, Ruiz-Mateos E, Marsh M, Saiardi A (2009) Inositol pyrophosphate mediated pyrophosphorylation of AP3B1 regulates HIV-1 Gag release. *Proc Natl Acad Sci USA* 106(50):21161–21166.
13. Chakraborty A, Kim S, Snyder SH (2011) Inositol pyrophosphates as mammalian cell signals. *Sci Signal* 4(188):re1.
14. Wundenberg T, Mayr GW (2012) Synthesis and biological actions of diphosphoinositol phosphates (inositol pyrophosphates), regulators of cell homeostasis. *Biol Chem* 393(9):979–998.
15. Wilson MS, Livermore TM, Saiardi A (2013) Inositol pyrophosphates: Between signalling and metabolism. *Biochem J* 452(3):369–379.
16. Szijgyarto Z, Garedew A, Azevedo C, Saiardi A (2011) Influence of inositol pyrophosphates on cellular energy dynamics. *Science* 334(6057):802–805.
17. Lonetti A, et al. (2011) Identification of an evolutionarily conserved family of inorganic polyphosphate endopolyphosphatases. *J Biol Chem* 286(37):31966–31974.
18. Saiardi A (2012) How inositol pyrophosphates control cellular phosphate homeostasis? *Adv Biol Regul* 52(2):351–359.
19. Illies C, et al. (2007) Requirement of inositol pyrophosphates for full exocytotic capacity in pancreatic beta cells. *Science* 318(5854):1299–1302.
20. Chakraborty A, et al. (2010) Inositol pyrophosphates inhibit Akt signaling, thereby regulating insulin sensitivity and weight gain. *Cell* 143(6):897–910.
21. Draskovic P, et al. (2008) Inositol hexakisphosphate kinase products contain diphosphate and triphosphate groups. *Chem Biol* 15(3):274–286.
22. Lin H, et al. (2009) Structural analysis and detection of biological inositol pyrophosphates reveal that the family of VIP/diphosphoinositol pentakisphosphate kinases are 1/3-kinases. *J Biol Chem* 284(3):1863–1872.
23. Saiardi A, Nagata E, Luo HR, Snowman AM, Snyder SH (2001) Identification and characterization of a novel inositol hexakisphosphate kinase. *J Biol Chem* 276(42): 39179–39185.
24. Bhandari R, Juluri KR, Resnick AC, Snyder SH (2008) Gene deletion of inositol hexakisphosphate kinase 1 reveals inositol pyrophosphate regulation of insulin secretion, growth, and spermiogenesis. *Proc Natl Acad Sci USA* 105(7):2349–2353.
25. Strahl BD, Allis CD (2000) The language of covalent histone modifications. *Nature* 403(6765):41–45.
26. Fischle W, Wang Y, Allis CD (2003) Binary switches and modification cassettes in histone biology and beyond. *Nature* 425(6957):475–479.
27. Bannister AJ, et al. (2005) Spatial distribution of di- and tri-methyl lysine 36 of histone H3 at active genes. *J Biol Chem* 280(18):17732–17736.
28. Lee J, Thompson JR, Botuyan MV, Mer G (2008) Distinct binding modes specify the recognition of methylated histones H3K4 and H4K20 by JMJD2A-tudor. *Nat Struct Mol Biol* 15(1):109–111.
29. Onnebo SM, Saiardi A (2009) Inositol pyrophosphates modulate hydrogen peroxide signalling. *Biochem J* 423(1):109–118.
30. Wissmann M, et al. (2007) Cooperative demethylation by JMJD2C and LSD1 promotes androgen receptor-dependent gene expression. *Nat Cell Biol* 9(3):347–353.
31. Ishimura A, et al. (2009) Jmjd2c histone demethylase enhances the expression of Mdm2 oncogene. *Biochem Biophys Res Commun* 389(2):366–371.
32. Sassone-Corsi P (2013) Physiology. When metabolism and epigenetics converge. *Science* 339(6116):148–150.
33. Wallace DC, Fan W (2010) Energetics, epigenetics, mitochondrial genetics. *Mitochondrion* 10(1):12–31.
34. Luo W, Chang R, Zhong J, Pandey A, Semenza GL (2012) Histone demethylase JMJD2C is a coactivator for hypoxia-inducible factor 1 that is required for breast cancer progression. *Proc Natl Acad Sci USA* 109(49):E3367–E3376.
35. Martelli AM, et al. (2011) Nuclear phosphoinositides and their roles in cell biology and disease. *Crit Rev Biochem Mol Biol* 46(5):436–457.
36. Irvine RF (2003) Nuclear lipid signalling. *Nat Rev Mol Cell Biol* 4(5):349–360.
37. Gozani O, et al. (2003) The PHD finger of the chromatin-associated protein ING2 functions as a nuclear phosphoinositide receptor. *Cell* 114(1):99–111.
38. Shi Y, Whetstine JR (2007) Dynamic regulation of histone lysine methylation by demethylases. *Mol Cell* 25(1):1–14.
39. Bannister AJ, et al. (2001) Selective recognition of methylated lysine 9 on histone H3 by the HP1 chromo domain. *Nature* 410(6824):120–124.
40. Trasler JM (2009) Epigenetics in spermatogenesis. *Mol Cell Endocrinol* 306(1–2): 33–36.
41. Peters AH, et al. (2001) Loss of the Suv39h histone methyltransferases impairs mammalian heterochromatin and genome stability. *Cell* 107(3):323–337.
42. Nishiyama M, et al. (2009) CHD8 suppresses p53-mediated apoptosis through histone H1 recruitment during early embryogenesis. *Nat Cell Biol* 11(2):172–182.
43. Riccio A, et al. (2006) A nitric oxide signaling pathway controls CREB-mediated gene expression in neurons. *Mol Cell* 21(2):283–294.